Journal of
Water, Sanitation & Hygiene for Development

 Journal of Water, Sanitation and Hygiene for Development Vol 11 No 6, 1071 doi: 10.2166/washdev.2021.105

Research Paper

Effect of single and combined exposures to UV-C and UV-A LEDs on the inactivation of *Klebsiella pneumoniae* and *Escherichia coli* in water disinfection

María-Angélica Galezzo* and Manuel Rodríguez Susa

Environmental Engineering Research Center, Department of Civil and Environmental Engineering, Universidad de los Andes, Carrera 1 No. 18A-12, Mario Laserna Building, Office 733, Bogotá, Colombia
*Corresponding author. E-mail: ma.galezzo@uniandes.edu.co

M-AG, 0000-0003-3945-7115; MRS, 0000-0002-8743-0200

ABSTRACT

A system consisting of one UV-A (365 nm) and two UV-C (265 nm) light-emitting diodes (LEDs) was built to evaluate the effect of single and combined exposures to UV-A and UV-C LEDs on *Klebsiella pneumoniae* and *Escherichia coli* inactivation and subsequent reactivation. The dose was measured by actinometry using potassium ferrioxalate. Of laboratory prepared samples, 10 mL were irradiated for 20, 30, 45, 60 and 90 s. Logarithmic inactivation and percentages of photoreactivation and dark repair were calculated. *E. coli* and *K. pneumoniae* were reduced by more than 7 and 4 logs, respectively, at a dose of 21.5 mJ cm^{-2} using UV-C. No positive synergistic effect on the inactivation of the two bacteria was observed when using a simultaneous combination of UV-C and UV-A, probably due to a reactivation of the bacteria in the presence of UV-A light, which was not observed in irradiated samples under an individual exposure of 265 nm. For *E. coli* under 265 nm, the percentage of photoreactivation amounted to 10%, 3 h after irradiation. The results of this study demonstrated the capacity to inactivate *E. coli* and *K. pneumoniae* up to a considerable level and provide information for the application of UV LEDs in point-of-use systems.

Key words: drinking water, *Klebsiella pneumoniae*, photo/dark repair, point-of-use systems, UV disinfection, water treatment

HIGHLIGHTS

- k_D was calculated for *K. pneumoniae*, under exposure to 265 nm UV light-emitting diode (LEDs).
- *K. pneumoniae* is more resistant than *E. coli* under 265 nm exposition.
- 265, 365 and 265/365 nm were effective to inactivate *E. coli* and *K. pneumoniae*.
- No positive synergistic effect for inactivation from the 265/365 nm LED combinations.
- Photoreactivation was the dominant mechanism of reactivation of *E. coli*.

GRAPHICAL ABSTRACT

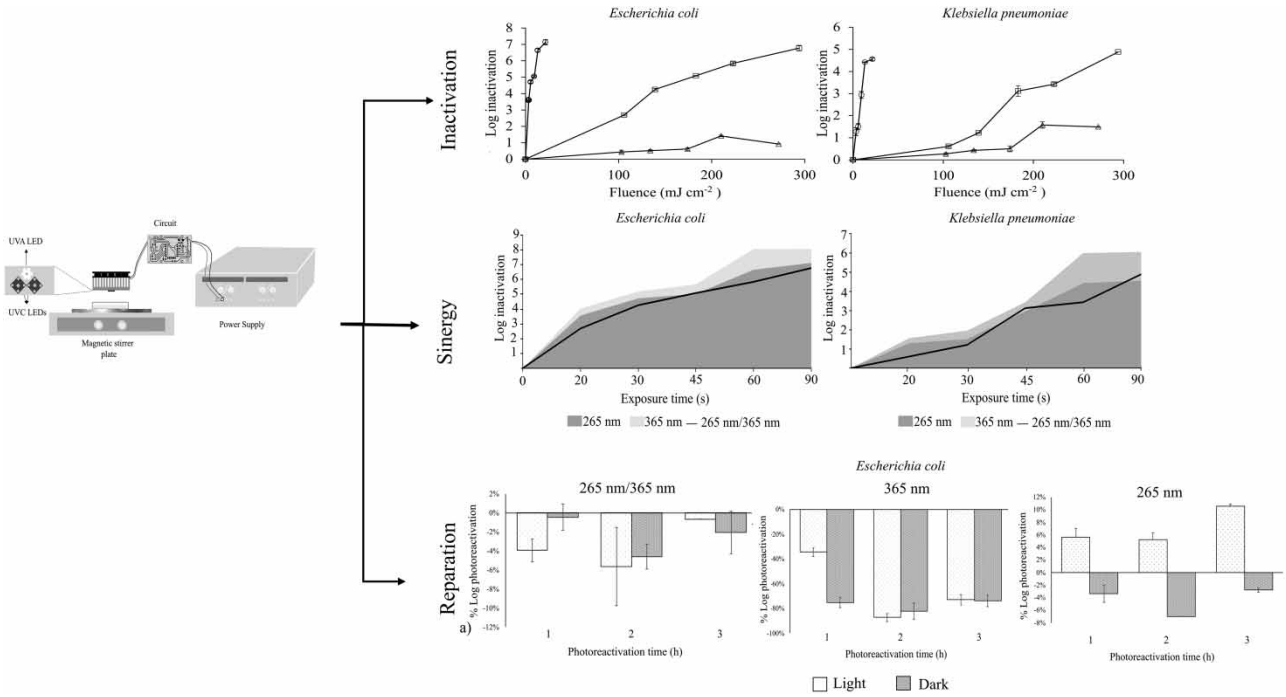

INTRODUCTION

Ultraviolet light emitted by medium- and low-pressure mercury lamps has been used as a water disinfection mechanism for over 50 years. Among its advantages is the fact that it does not generate overdose, disinfection by-products, toxins or volatile organic compounds, and it does not alter the smell and taste of water. However, due to its fragility, high energy consumption, final disposal and high running cost (Chatterley & Linden 2010), it is a technology that is not easily applicable to some contexts, particularly remote communities.

In recent decades, mercury-free and longer-lasting light-emitting diodes (LEDs) have been manufactured with wavelengths in the ultraviolet light range (100–400 nm). Their small size and wide wavelength range make them easy to configure into many different arrays. Several studies have been conducted to assess LED inactivation efficacy and found that this varies according to multiple factors including wavelength, type of microorganism, water quality, fluence rate and system hydraulic conditions (Blatchley *et al.* 2008; Würtele *et al.* 2011). However, as with traditional UV light technology, subsequent repair after UV light inactivation has been evident, mainly by means of photoreactivation and dark repair processes (Rastogi *et al.* 2010). A number of different authors have combined wavelengths to improve inactivation efficacy and eliminate or decrease repair processes by simultaneously or sequentially combining different wavelengths. Chevremont *et al.* (2012) combined UV-A (365 and 405 nm) and UV-C (254 and 280 nm), finding that there is greater efficiency in microbial inactivation of fecal indicators (mesophilic bacteria, fecal enterococci and fecal coliforms) when used simultaneously than when used separately, a result similar to that of Nakahashi *et al.* (2014), who combined wavelengths of 254 and 365 nm to inactivate *Vibrio parahaemolyticus*.

Several microorganisms have been extensively evaluated, among which stand out *Escherichia coli*, *Bacillus subtilis*, *Pseudomonas aeruginosa* and *MS-2*. However, these have been evaluated with low doses so far. In this study, higher irradiation doses were used to evaluate the inactivation of *E. coli*, a microbiological indicator of water quality widely used around the world, and *Klebsiella pneumoniae*, an opportunistic, resistant pathogen that can easily form biofilms on pipe walls and/or water storage tanks, which can be of great interest especially in point-of-use systems for rural communities to prevent biofilm formation. *K. pneumoniae* occurs naturally in water sources, wastewater, soil and plants (Foka *et al.* 2018; Dang *et al.* 2020; Voigt *et al.* 2020). It can cause urinary tract infections and pneumonia, mainly in people with weak immune systems or existing diseases. Despite this, the bacterium's reaction to UV light has been very sparsely studied (Giese & Darby 2000). The purpose of

this research was to study inactivation and subsequent repair behavior, under single and combined exposures of *E. coli* and *K. pneumoniae* to UV-C (265 nm) and UV-A (365 nm) LEDs to evaluate the applicability for point-of-use systems.

METHODS

UV-LED batch system configuration

A system was built with two 265 nm UV-C LEDs (KL265-50T-SM-WDM2) and one 365 nm UV-A LED (HYR35X43B365KN-D1) with a maximum optical power of 60 mW at 500 mA and 1,500 mW at 700 mA, respectively. 265 nm LEDs were used because at the time of the study, the LEDs with the highest power on the market in the UV-C range corresponded to this wavelength. We worked with a single UV-A LED because the power of this LED (1,500 mW) was high enough in contrast to the power of the UV-C LED (60 mW) used. The technical characteristics of these LEDs are detailed in Supplementary Material, Appendix A.

A circuit was designed with three resistors connected in parallel. For voltage and current control, a trimmer, a capacitor and a transistor for each LED were installed. Three additional switches were installed for independent power-up, and an external power supply was used to operate the disinfection module.

LED lifespan depends partly on how the operating temperature is managed, given that the electrical energy applied to the LEDs is transformed into light and heat. Thus, an increase in temperature decreases the light emitted. Accordingly, the LEDs were anchored with screws to a heatsink, heatsink paste was applied, and a 12 V fan was installed. The voltage and current of each LED were measured using a multimeter (Peak Teach® 3725). The temperature was measured using an infrared thermometer in each LED, the printed circuit board (PCB) and the heatsink. The laboratory temperature was also reported (Table 1).

Irradiance measurement

The irradiance emitted by each LED was measured by chemical actinometry (Supplementary Material, Appendix B). For this study, the Hatchard-Parker actinometer was used. This actinometer is applied for a wide range of wavelengths (250–500 nm), among which we have the two lengths of interest (265 and 365 nm).

For the actinometric tests, 10 mL of actinometric solution was poured into a Petri dish with a diameter of 8.8 cm, which was then placed on a stir plate at 500 rpm and 2 cm from the light source, in order to obtain a homogeneous distribution of the solution (Figure 1). This dish was irradiated for 20, 30, 45, 60 and 90 s under the light of: (i) two 265 nm LEDs, (ii) one 365 nm LED and (iii) the combination of the above LEDs. For each experiment, the actinometric solution was changed in order to reduce the uncertainty in the production of ferrous ions (Fe^{2+}). The unirradiated solution was taken as a target. 1 mL of the blank solution and of each irradiated sample were poured into 100 mL volumetric balloons, to which 5 mL of buffer solution and 3 mL of 0.2% w/v 1,10-phenanthroline solution were added. Each solution was measured for absorbance at 510 nm in a spectrophotometer (UV-VIS Genesys™ 10 Bio, THERMO).

Details of the irradiance calculation can be found in Supplementary Material, Appendix B. The quantum yield ($\phi_{AC,\lambda}$) used for the UV-A LED (365 nm) tests was 1.18 and 1.23 for UV-C LEDs (265 nm).

Inoculum preparation

E. coli (ATCC 25922™) and *K. pneumoniae* colonies (isolated from Bogotá's Municipal Wastewater Treatment Plant and tested by DNA extraction in the Environmental Laboratory at Universidad de los Andes) were taken from EMB (Eosyn Methylene Blue Agar) and MacConkey plates, respectively, after incubation (Binder BD 53 L) for 24 h at 37 ± 1 °C and added to 90 mL of sterile TSB (Tryptic Soy Broth). This solution was placed in a shaker at 37 ± 1 °C and 200 rpm in

Table 1 | System operating conditions

LED (nm)	Voltage (V)	Current (mA)	T_{LED} (°C)	T_{PCB} (°C)	T_{Hsk} (°C)[a]	T_{Room} (°C)[a]
265	7.2	500	47.7	39.76	31.3	18
265	7.2	490	64.2	67.1		
365	3.8	600	45.9	50.6		

T_{LED}, LED temperature; T_{PCB}, PCB temperature; T_{Hsk}, Heatsink temperature.
[a]Room and heatsink temperatures were the same for the whole system.

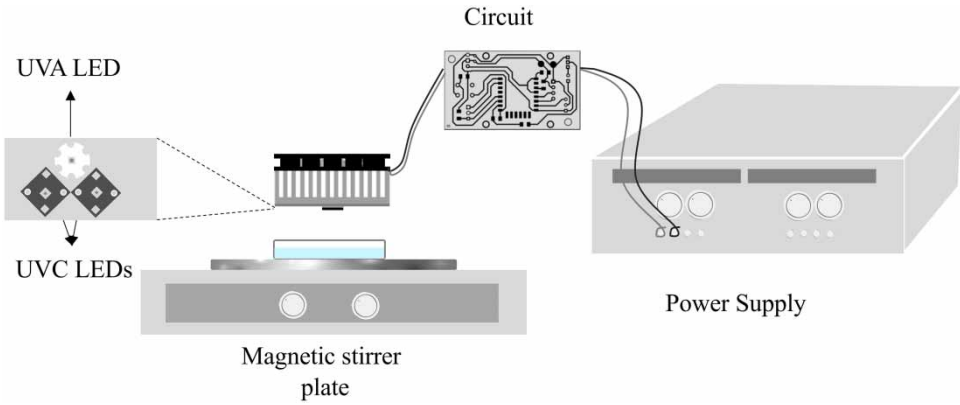

Figure 1 | Diagram of UV disinfection reactor.

order to incubate. Every 30 min the optical density (OD) was measured in a spectrophotometer (NanoDropTM 2000, THERMO) at 600 nm until reaching an exponential phase with an OD of 1.0. The target solution was established using sterile TSB. Cells were collected by centrifugation (Sorvall™ Legend™ XFR, THERMO) at 5,000 g for 10 min; washed three times with PBS (phosphate buffered saline; pH 7.4) and then suspended in PBS to a concentration between 10^6 and 10^8 CFU/mL, determined by plate count (Petrifilm™). New solutions were prepared each time a new test was performed.

Inactivation experiments

10 mL of solution were placed in an 8.8 cm diameter Petri dish, which was placed on a magnetic stirrer plate at 500 rpm. The solution was irradiated for 20, 30, 45, 60 and 90 s by single and combined 265 and 365 nm LEDs. For each exposure, the sample of 10 mL was changed to avoid measurement uncertainty.

Before and after irradiation, 1 mL of the sample was diluted and seeded in Petrifilm™ EC plates for *E. coli* and Petrifilm™ CC for *K. pneumoniae* and incubated at 37 ± 1 °C before the bacteria count. Each experiment was performed in triplicate. Plates with valid dilutions were those with between 1 and 300 colonies. Sterile water was used for the dilutions. The number of bacteria was expressed in CFU/mL.

Reactivation experiments

The *E. coli* repair process was evaluated for samples irradiated for 90 s. After UV irradiation, 4.5 mL of the sample was transferred to a Petri dish, which was placed in front (2 cm) of a 20 W LED light to evaluate the photorepair, with a light intensity of 12,160 Lx (Luminometer UT380). 1 mL of this solution was analyzed every hour for a period of 3 h. The remaining 4.5 mL of the radiated sample was placed in aluminum foil-wrapped Petri dishes to prevent light from passing through and therefore assess dark repair. The repair time was selected based on previous studies that indicated that the maximum levels of photorepair are reached between 2 and 3 h before stabilization (Zimmer & Slawson 2002; Hu *et al.* 2005).

Reactivations were performed at room temperature (18 °C), which is independent of the photoreactivation rate (Quek & Hu 2008). The procedure used to determine colonies by dark repair was the same as that used to evaluate photorepair. The samples were diluted, seeded, incubated in triplicate and analyzed using the Petrifilm™ plate count method.

Data analysis

The result for each test was the average of the values obtained in the triplicate. The value was expressed in colony-forming units per milliliter (CFU/ml). The disinfection efficacy was evaluated through log reduction, calculated for each trial using Equation (1). The log reduction versus the exposure time and fluence was plotted.

$$\text{Inactivation Log} = \text{Log}_{10}\left(\frac{N_0}{N}\right) \tag{1}$$

where N_0 is the concentration of microorganisms before exposure to a UV dose, and N is the concentration of microorganisms after exposure.

The inactivation rate for each microorganism depends on the UV fluence, which is described based on a first-order model (Equation (2)), where there is a linear relationship between logarithmic inactivation and UV dose or fluence.

$$\ln \frac{N}{N_0} = -k_D \cdot \mathrm{D} \tag{2}$$

where D is the dose in mJ cm^{-2}, and k_D is the constant inactivation rate.

Typically, inactivation at low fluence rates increases slightly producing a shoulder. Although the causes of this phenomenon are still under investigation, some hypotheses relate it to a process of agglomeration, experimental biases, or hydraulic effects (Würtele *et al.* 2011). After an offset fluence, inactivation starts in a log-linear relationship, sometimes followed by a tailing phase at higher fluences, probably because the resynthesis rate of the microorganism's vital components reaches a higher level than the destruction rate (Mossel *et al.* 1995). Where a shoulder appears in the inactivation plot, the shoulder model described in Equation (3) can be applied, where b is the y-axis intercept.

$$\log\left(\frac{N_0}{N}\right) = k_D * \mathrm{Dosis} - b \tag{3}$$

In this study, the constant inactivation rates were calculated for the Chick–Watson and shoulder models. For the first, only the data from the linear region were used and for the second model, the data from the linear and shoulder regions were used. Additionally, regressions were developed for three models: first-order linear, second-order polynomial and logarithmic with the totality of the data, in order to find a better fit when calculating the flows corresponding to the desired logarithmic inactivation.

The synergistic effect of combined wavelengths on microorganism inactivation was evaluated using a paired sample t-test to compare the logarithmic inactivation of the combined LEDs (265/365 nm) and the sum of the logarithmic inactivation of each individual LED (265 +365 nm).

Photorepair and dark repair efficiency was calculated using the following equation:

$$\text{Log repair percentage (\%)} = \frac{\text{Log inactivation}_o - \text{Log inactivatio}_t}{\text{Log inactivation}_o} \cdot 100\% \tag{4}$$

where Log inactivation$_o$ is the log reduction presented immediately after UV radiation, and Log inactivation$_t$ is the log reduction presented after UV radiation in a period t of repair.

Two-way repeated measurement ANOVA tests were developed to compare the two factors studied (wavelength and reactivation time) and their three levels (wavelength: 265, 365 and 265/365 nm; time: 1, 2 and 3 h). Paired sample t-tests were conducted to compare the two types of repairs depending on the type of exposure. All graphs were created in Microsoft Excel®, and statistical data analysis was performed in Stata® version 12 (Stata Corp.) and SPSS® version 21 (IBM).

RESULTS

Actinometry

The results of the OD reading for iron sulfate heptahydrate solution ($FeSO_4 \cdot 7H_2O$) were plotted against Fe^{2+} concentration. The R^2 obtained in the calibration was 0.9996, and the molar absorption coefficient of the phenanthroline-Fe^{2+} compound, which is equivalent to the slope of the equation of the line, was $\varepsilon_{Fe^{2+}} = 11{,}076$ l mol^{-1} cm^{-1}, which was used to calculate LED fluence.

The average irradiance emitted was 0.20 ± 0.03 mW cm^{-2} for the two 265 nm LEDs and 4.0 ± 0.83 mW cm^{-2} for the 365 nm LED. Results from tests are shown in Figure 2, where the irradiance was averaged over the time used in the inactivation trials, and the time was measured since LEDs were turned on. The irradiance varied depending on how long it is turned on. While for the 265 nm LEDs, the irradiance increased until reaching equilibrium, for the 365 nm LED, the irradiance decreased until reaching close to this equilibrium.

Each wavelength was treated with a different regression model. The average fluence rate was calculated using the resulting model equations, as shown in Table 2. The dose for the 265/365 nm combination was calculated by adding the doses of the single LEDs.

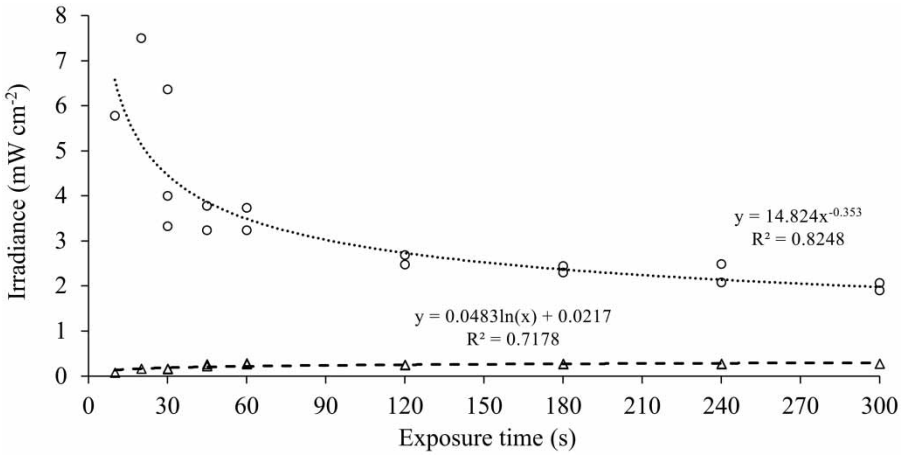

Figure 2 | Irradiance for each LED as a function of exposure time: (○) 365 and (Δ) 265 nm.

Table 2 | Average dose emitted for each LED configuration

Radiation time (s)	$Dose_{265\ nm}$ (mJ cm^{-2})[a]	$Dose_{365\ nm}$ (mJ cm^{-2})	$Dose_{265\ nm+365\ nm}$ (mJ cm^{-2})
20	3.3	103.0	106.3
30	5.6	133.9	139.4
45	9.3	174.0	183.3
60	13.2	209.6	222.8
90	21.5	272.5	294.0

[a]This corresponds to the total dose for both LEDs UV-C (265 nm).

Microbial inactivation

The concentration of bacteria in the inoculated solution varied between 10^6 and 10^8 CFU/ml. Inactivation profiles of *E. coli* and *K. pneumoniae* as a function of exposure time and fluence for different wavelengths are shown in Figure 3.

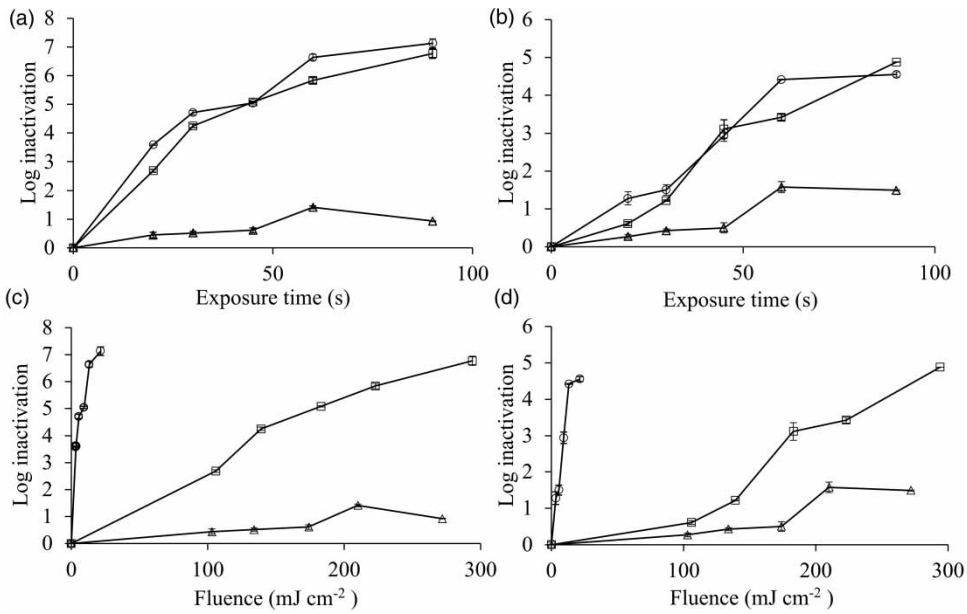

Figure 3 | Inactivation profile as a function of exposure time for (a) *E. coli*, (b) *K. pneumoniae* and depending on the fluence for (c) *E. coli* and (d) *K. pneumoniae* under exposure to (○) 265, (Δ) 365, (□) 265/365 nm.

Modeling results using linear, logarithmic and second-order polynomial regression were assessed. R^2 values were calculated and compared for the three models (Table 3). The second-order polynomial and logarithmic models fit the data better than the linear model. The second-order polynomial model was best suited for *E. coli* under all three types of UV-LED exposure and for *K. pneumoniae* under UV-A LED exposure (265 nm), while the logarithmic model was best suited for *K. pneumoniae* under UV-C LED exposure (265 nm) and the combination of UV-A and UV-C LEDs (265/365 nm). Lower R^2 was obtained for the inactivation curves under exposure to 365 nm due to atypical inactivation values at 210 mJ cm^{-2}. This effect probably may be related to the resynthesis rate of the vital components of microorganisms which reaches a higher level than the destruction rate (Giese & Darby 2000). It is necessary for future studies to evaluate the inactivation in a longer exposure time to determine if it corresponds to a tailing region.

To calculate the sensitivity of the microorganisms, described by the constant rate of inactivation k_D (cm^2 mJ^{-1}), new linear regressions were developed for the points that were within the linear region of the inactivation graph under exposure to 265 and 265/365 nm, excluding those that were part of the shoulder or tailing region, while under exposure to the 365 nm LED, the atypical data corresponding to 210 mW cm^{-2} were omitted. The calculated inactivation constants are shown in Tables 4 and 5.

The value of k_D at 265 nm when applying the Chick–Watson model was 0.45 $\pm$ 0.11 cm^2 mJ^{-1}, and this value decreased when considering the shoulder model (0.28 $\pm$ 0.05 cm^2 mJ^{-1}). With respect to *K. pneumoniae* when applying the Chick–Watson model and the shoulder model, the k_D value at 265 nm was 0.33 cm^2 mJ^{-1}.

Minor log reductions of *K. pneumoniae* show that it has a higher resistance than *E. coli* under the same exposure conditions at 265 nm ($p = 0.006$) and 265/365 nm ($p = 0.006$), while under exposure to 365 nm, the logarithmic inactivation of *E. coli* and *K. pneumoniae* showed no statistically significant difference (paired sample *t*-test $p = 0.6153$).

This study reached a maximum logarithmic inactivation of 7.13 $\pm$ 0.16 for *E. coli* and of 4.55 $\pm$ 0.07 for *K. pneumoniae* under exposure to 265 nm.

Evaluation of the synergetic effect

Figure 4 shows the logarithmic inactivation of *E. coli* and *K. pneumoniae*, for the combination of the single exposures to 265 and 365 nm (area) and for the simultaneous exposure to 265/365 nm (line). The sum of the logarithmic inactivation of *E. coli* under the single exposure to 265 and 365 nm showed statistically significant differences ($p = 0.018$) when compared to the

Table 3 | Logarithmic inactivation (Y) as a function of fluence (X)

	Second order polynomial		Logarithmic		Linear	
UV source (nm)	R^2	Equation	R^2	Equation	R^2	Equation
E. coli						
265	0.9455	$Y = -0.0208X^2 + 0.7452X + 0.6093$	0.9469	$Y = 1.932\text{In}(X) + 1.2537$	0.7697	$Y = 0.2912X + 1.95\ 32$
365	0.7158	$Y = -6\text{E} - 06X^2 + 0.006X - 0.0507$	0.5096	$Y = 0.7505\text{In}(X) - 3.0672$	0.7024	$Y = 0.0043X + 0.0159$
265/365	0.9894	$Y = -4\text{E} - 05X^2 + 0.0344X - 0.0933$	0.9847	$Y = 3.8913\text{In}(X) - 15.229$	0.9661	$Y = 0.0237X + 0.367$
K. pneumoniae						
265	0.9661	$Y = -0.0102X^2 + 0.4448X - 0.1733$	0.9104	$Y = 2.02641\text{In}(X) - 1.4357$	0.8839	$Y = 0.223X + 0.4834$
365	0.8267	$Y = 2\text{E} - 05X^2 + 0.0019X - 0.0447$	0.7760	$Y = 1.4587\text{In}(X) - 6.6281$	0.7810	$Y = 0.0062X + 0.2144$
265/365	0.9493	$Y = 3\text{E} - 05X^2 + 0.0078X - 0.1702$	0.9723	$Y = 4.2897\text{In}(X) - 19.57$	0.9151	$Y = 0.0178X - 0.5994$

Table 4 | Kinetic parameters of the linear Chick–Watson model applied to the linear region of *E. coli* and *K. pneumoniae*

	E. coli				*K. pneumoniae*			
UV source (nm)	k_D (cm^2 mJ^{-1}) $\pm$ SD	R^2	*p*-value	CI	k_D (cm^2 mJ^{-1}) $\pm$ SD	R^2	*p*-value	CI
265	0.4471 $\pm$ 0.1065	0.85	0.025	0.1081–0.7861	0.3274 $\pm$ 0.0274	0.99	0.001	0.2543–0.4004
365	0.0033 $\pm$ 0.0002	0.99	0.001	0.0026–0.0041	0.0053 $\pm$ 0.0012	0.87	0.020	0.0016–0.0090
265/365	0.0270 $\pm$ 0.0019	0.99	0.001	0.0209–0.0331	0.0178 $\pm$ 0.0027	0.92	0.003	0.0103–0.0254

SD, standard deviation; CI, confidence interval.

Table 5 | Kinetic parameters of the shoulder model applied in inactivation experiments for *E. coli* and *K. pneumoniae*

	E. coli					*K. pneumoniae*				
UV source	**k_D (cm² mJ⁻¹) ± SD**	***b***	***R²***	***p*-value**	**CI**	**k_D (cm² mJ⁻¹) ± SD**	***b***	***R²***	***p*-value**	**CI**
265	0.2816 ± 0.0499	2.7878	0.94	0.030	0.0666–0.4966	0.3331 ± 0.0383	−0.0631	0.97	0.013	0.1665–0.4957
365	0.0029 ± 0.0002	0.1304	0.99	0.003	0.0022–0.0036	0.0073 ± 0.0013	−0.5742	0.94	0.029	0.0018–0.1282
265/365	0.0257 ± 0.0044	0.2816	0.94	0.028	0.0067–0.0447	0.0231 ± 0.0027	−1.7102	0.96	0.004	0.0143–0.0318

SD, Standard deviation; CI, Confidence interval.

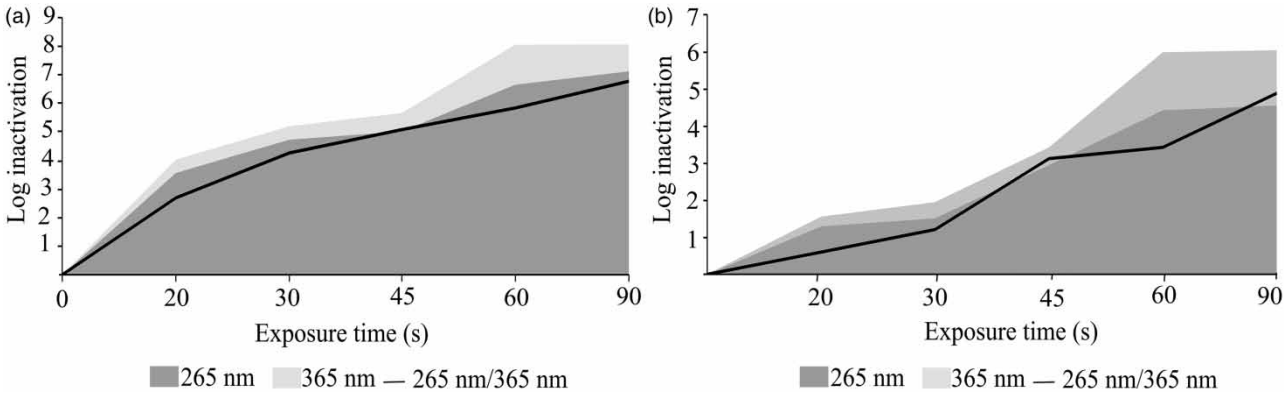

Figure 4 | Logarithmic inactivation comparison between addition of single wavelengths (265 + 365 nm) and simultaneous combination of 265/365 nm for (a) *E. coli* and (b) *K. pneumoniae*.

logarithmic inactivation of simultaneous exposure to 265/365 nm, inactivation being greater when the single exposures of UV-A and UV-C LEDs are added (5.17 ± 3.00) which indicates that there was no positive synergistic effect in the inactivation of the irradiated samples under simultaneous exposure of UV-A and UV-C LEDs (4.11 ± 2.45). Additionally, statistically significant differences were observed between logarithmic inactivation of *E. coli* under 265 nm single exposure (4.50 ± 2.57) and simultaneous 265/365 nm exposure ($p = 0.049$) with a higher level of inactivation by single exposure to 265 nm.

For *K. pneumoniae*, there were also statistically significant differences in inactivation by simultaneous exposure to 265/365 nm (3.16 ± 2.47) compared to the inactivation sum of single exposures to 265 and 365 nm (2.21 ± 1.89) ($p = 0.048$), indicating that there was greater inactivation when using LEDs single rather than using them simultaneously. However, no statistically significant difference ($p = 0.299$) was observed when comparing logarithmic inactivation by single exposure to 265 nm (2.45 ± 1.83) and combined exposure to 265/365 nm. Results show that there was no positive synergistic effect when combining 265/365 nm in the inactivation of *K. pneumoniae*.

Bacterial repair evaluation

The logarithmic percentages of photoreactivation and dark repair for *E. coli* under single and combined exposures to radiation from UV-A and UV-C LEDs are presented in Figure 5. Photoreactivation was only observed in samples exposed to 265 nm LEDs. No statistically significant differences in the percentage of logarithmic photoreactivation are observed during the 3 h of evaluation ($p > 0.05$). No dark repair is observed in any of the three exposures during the time studied. Negative photoreparation and dark reparation were observed under all three exposures with inactivation percentages close to 90% under 365 nm exposure.

DISCUSSION

The results of this study show that 265 nm LEDs have a great germicidal power on *E. coli* and *K. pneumoniae*, reaching a logarithmic inactivation rate greater than 7 and 4 logs, respectively. These values satisfy the high protection target (4 logs) suggested by the WHO for domestic water treatment. The findings, therefore, support that involving UV LEDs in future water treatment designs can maximize the application of UV dose and reduce the bacterial load to levels safe for human consumption. Likewise, this technology can be a disinfection alternative for remote places such as rural areas.

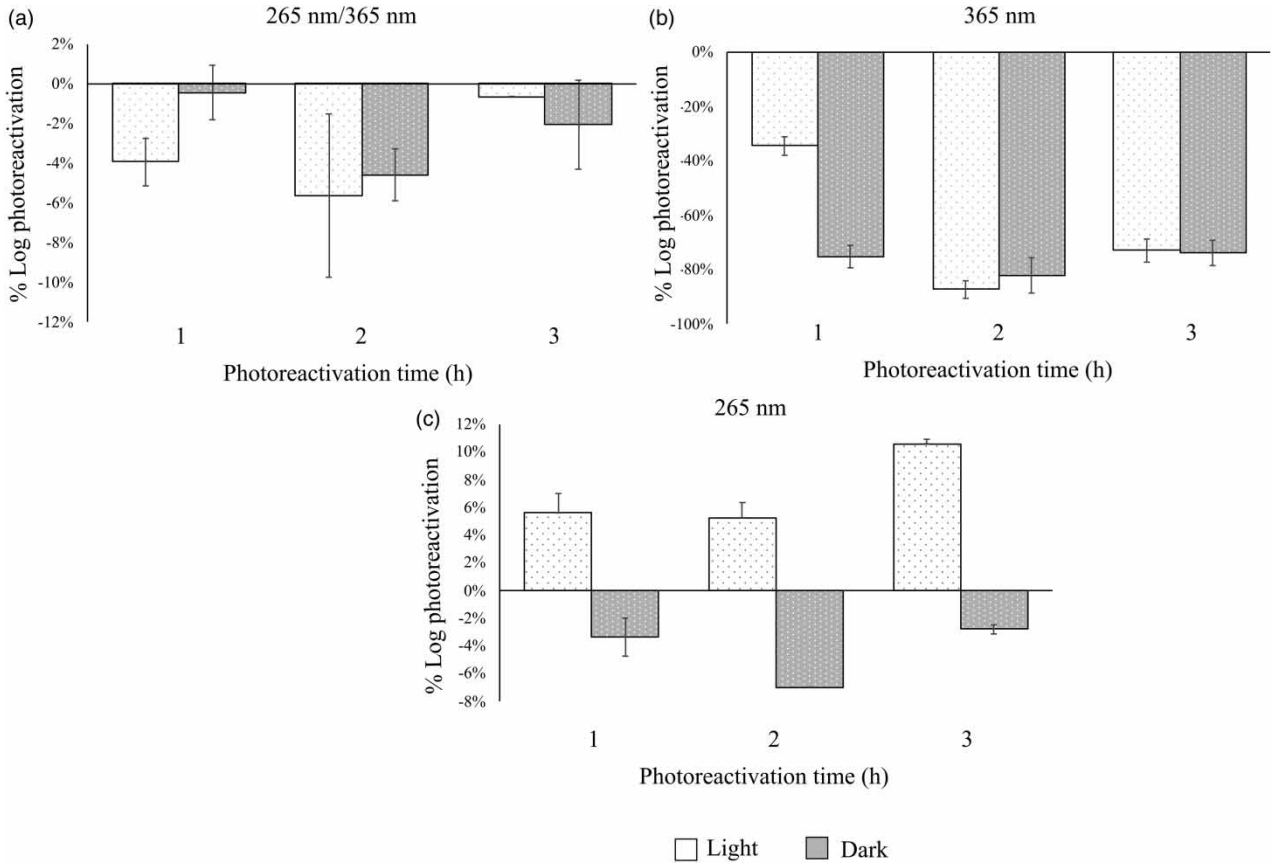

Figure 5 | Percentages of photo-reactivation and dark repair of *Escherichia coli* under exposure to: a) 265/365 nm, b) 365 nm, c) 265 nm

The constant inactivation rate (k_D) equal to 0.45 cm mJ^{-1} for *E. coli* when applying the Chick–Watson model was close to that reported by Oguma *et al.* (2013) (0.43) and by Li *et al.* (2017) (0.41 $\pm$ 0.029), who used the same wavelength to inactivate *E. coli* even though the LED configuration was arranged in a different way. While the shoulder model yielded a value of 0.28 cm^2 mJ^{-1}, similar to that reported by Chatterley & Linden (2009) (0.287) in the linear portion of the inactivation curve. However, the two inactivation rates obtained were much lower than the value reported by Rattanakul & Oguma (2018) (0.80 $\pm$ 0.06). Differences in inactivation rate values may be associated with different experimental settings, the *E. coli* strain used, sample preparation conditions, fluence calculation and/or different system settings.

On the other hand, *K. pneumoniae* obtained a lower constant inactivation rate (k_D), at 0.33 cm^2 mJ^{-1} for both the Chick–Watson model and the shoulder model. To date, no studies have evaluated this bacterium under single exposure to 265 nm or the simultaneous combination of 265/365 nm. Nevertheless, Giese & Darby (2000) evaluated this same bacteria under 254 and 280 nm, reporting inactivation rates of 0.42 and 0.30 cm^2 mJ^{-1}, respectively.

The logarithmic inactivation of *E. coli* and *K. pneumoniae* under 365 nm was low, which can be explained because this wavelength reaches 1 log reduction when applying doses close to 60,000 mJ cm^{-2}. Given that in this study, UV-A (365 nm) is used to assess the synergistic effect with UV-C (265 nm) on inactivation and subsequent reactivation, and the individual results are not considered in detail.

No positive synergistic effect was observed in the inactivation of the studied bacteria when simultaneously combining 265/365 nm. On the contrary, there was a reduction in the inactivation when comparing the combined and simultaneous effect of 265/365 nm with the sum of 265 + 365 nm individually, as well as for single exposure to 265 nm in the case of *E. coli*. A decrease in the inactivation of this bacterium was also recently reported by Song *et al.* (2018). Reduced logarithmic inactivation with UV-A light may be related to the photoreactivation, by which DNA damage is restored, either by simultaneous or subsequent irradiation of ultraviolet or near-visible light. DNA damage is repaired by the photolyase enzyme, which is generated by visible/blue light (370–500 nm) and protects the genome from harmful effects by advancing rapidly in a matter

of nanoseconds (Essen & Klar 2006). However, the photolyase can, in turn, be degraded in the presence of UV-C light under fluences greater than 25 μW cm^{-2} (Zhang *et al.* 2007). Further studies are required to corroborate whether the rate of photolyase enzyme generation in the presence of UV-A light is higher than the degradation rate in the presence of UV-C light in such a way that it can be inferred whether part of the DNA damage caused by LED exposure to 265 nm to *E. coli* and *K. pneumoniae* bacteria could have been countered by simultaneous irradiation with 365 nm UV light, which is part of the near-UV light spectrum.

In contrast to the results obtained concerning synergy, some authors (Chevremont *et al.* 2012; Nakahashi *et al.* 2014) report a synergistic effect when irradiating *E. coli* contaminated water samples under a simultaneous combination of UV-A and UV-C. However, these authors evaluated the synergistic effect in different experimental settings, with different combinations of wavelengths and different types of bacteria. Chevremont *et al.* (2012), for example, worked with a water sample from a highly turbid wastewater effluent, which may have influenced the reduced photoreactivation of DNA damage caused by UV-C radiation. As for the second study, in addition to working with a different bacterium (*V. parahaemolyticus*), the fluence provided by the LED-UV-A was much higher (70 mW cm^{-2}) than the one used in this study (4 mW cm^{-2}), which could generate a greater contribution to the logarithmic inactivation of the bacteria by the UV-A light. Based on the results of this study, the simultaneous use of these wavelengths (265/365 nm) is not recommended when the UV-A dose is not high enough to guarantee a positive contribution to the inactivation of the bacteria by counteracting their repairing power.

When evaluating repair in *E. coli*, photoreactivation was only observed for samples irradiated at 265 nm, while dark repair was not detected for any of the three levels of exposure. This is consistent with the theory of photoreactivation in which the photolyase enzyme acts as a repair agent for DNA damage known as CPDs (Cyclobutane Pyrimidine Dimers) and 6–4 PPs (photoproducts). These are induced most efficiently by radiation at about 260 nm (Britt 1996), while their formation in the presence of UV-A light is almost negligible. The absence of photoreactivation in samples exposed to combined 265/365 nm radiation during the first 3 h of the study could be associated with the fact that the few reparable DNA damages caused by UV-C radiation (265 nm) were repaired during simultaneous UV-A radiation (365 nm).

The lower percentage values of *E. coli* photoreactivation compared to other studies (Li *et al.* 2017; Xiao *et al.* 2018) may be related to higher doses used in the present study (21 mJ cm^{-2}), since higher doses induce higher DNA damage and they decrease repair power. Although the repair rate may increase over a longer period, previous studies show that the highest reactivation rate is reached after 2–3 h, and that after this time, the rate decreases, reaching its minimum value (Zimmer & Slawson 2002; Hu *et al.* 2005).

The perceived lack of dark repair is consistent, since this type of repair occurs at a lower frequency than the photoreactivation process (Guo *et al.* 2011). Although negative repair was observed under all three exposures during the 3 h of evaluation, it reached inactivation percentages close to 90% under 365 nm exposure, a phenomenon that Nyangaresi *et al.* (2018) attributed to a residual effect on the DNA of bacteria and that is independent of wavelength and fluence. However, it is important that in future studies, this phenomenon can be analyzed given the differences attributed to the wavelength of 365 nm observed here. Early inactivation in our study may also be influenced by a higher exposure dose.

Bearing in mind that the inactivation process is followed by subsequent repair, it is important to consider repair percentages when designing disinfection systems. Under the conditions established for the study, photoreactivation is the dominant mechanism. Thus, in order to inactivate *E. coli* with a dose of 21.5 mJ cm^{-2} under exposure to 265 nm and without considering the photoreactivation phenomenon, a logarithmic inactivation of 7.13 $\pm$ 0.16 can be reached. However, when considering the photoreactivation process, inactivation can be reduced by about 10 to 6.4%. By combining 265 and 365 nm LEDs, the logarithmic inactivation was lower (6.7 $\pm$ 0.17); however, during the 3 h evaluated, there was no photoreactivation process, but instead a continuity of inactivation was observed. This interesting phenomenon should be evaluated more widely, since it could vary according to the organisms and the wavelengths evaluated.

On the other hand, as far as the technical part of the LEDs is concerned, the variation in irradiance over time could be related to temperature management, which varies over time by modifying the optical energy emitted, like the warm-up phenomenon in UV lamps, but with much faster stabilization in time. While in UV lamps the radiation, stabilization is in the order of 7–10 min, for the evaluated LEDs, it is around 45 s for UV-A and close to 4 min for UV-C. It is important for disinfection systems to be designed with this variation in mind, either by recirculating exposed water during the irradiance stabilization time or by designing circuits that allow for stable irradiance once the device is turned on.

This study presents some limitations. The behavior of UV LEDs is different from UV lamps in terms of the type of radiation, and protocols designed for the latter are not compatible with UV LEDs, mainly due to the different way the light beam travels from lamps and from LEDs; therefore, experimental configurations may vary between studies. We were not carried out

control tests to verify the effect of other operating conditions such as pH, temperature or inactivation rates. The results presented here should be validated for field use considering the hydraulic configurations of the reactor to be designed.

Finally, the reported findings provide relevant information to aid the construction of disinfection systems where the use of UV LEDs is required, given that the dose of each system will depend on the microorganism of interest and the wavelength to be used. Even though the UV-C LED used was the most powerful available on the market, it is still a low power; however, only two LEDs provided considerable logarithmic inactivation. Given the efficiency of these LEDs in bacterial inactivation, they can be a viable solution for household water treatment, especially in rural configurations where conventional water purification systems are difficult to install. For this, it is required that the water to be treated had low turbidity, it is recommended to use it in conjunction with a previous turbidity removal treatment, either use of filters or coagulants. The use of UV LEDs has advantages over chlorination, which is the widely used method for disinfection, shorter contact times, no generation of by-products, and there will be no chemical overdoses. However, currently, the power of UV-C LEDs is still low and the costs for implementation are high. The power emitted by UV-C LEDs is expected to increase and their cost to decrease in the short term in order to ensure their sustainability in said context.

It is recommended for future studies to evaluate the subsequent reparation of *K. pneumoniae*, considering that this phenomenon is not only influenced by physical processes associated with the dose but also by biological processes that vary with each microorganism. Given that *K. pneumoniae* was more resistant than *E. coli* to the wavelength studied (265 nm), it can also be used as a bacterial indicator when evaluating disinfection efficacy in systems that use this type of technology. This guarantees greater microbiological protection.

CONCLUSIONS

Single and combined commercially available UV-A (365 nm) and UV-C (265 nm) LEDs were used to study *E. coli* (ATCC 25922) and *K. pneumoniae* inactivation in a batch disinfection system. The results indicate that UV-C LEDs (265) are effective in inactivating *E. coli* and *K. pneumoniae*.

Statistically significant differences between the logarithmic inactivation of *E. coli* and *K. pneumoniae* make the latter more resistant to the wavelength evaluated, which was also supported by a higher k_D calculated for *E. coli*.

No synergistic effect on the inactivation of the two bacteria was observed when simultaneously combining 265 and 365 nm waves. Combined emissions of 265/365 nm showed less inactivation efficacy than emissions from separately applied components. Despite the high inactivation rates achieved, photoreactivation by *E. coli* reached 10% during the hours following irradiation. However, no dark repair was observed with the single or combined simultaneous use of 265 and 365 nm. Low percentage values of *E. coli* photoreactivation may be related to higher doses used for inactivation.

Taking into account the results obtained in this study, in point-of-use systems the subsequent use of a disinfectant can be eliminated, by implementing UV-C LEDs or the combination of UV-C/UV-A LEDs, which may be a disinfection option with an inactivation dose that considers the percentage of photoreactivation together with storage in the absence of light.

AUTHOR CONTRIBUTIONS

The research proposal, the design and development of the methodology, the analysis of data, the interpretation of results and the draft version were developed by María-Angélica Galezzo. Manuel Rodríguez Susa. reviewed the research proposal, contributed to the design of the methodology, reviewed, commented and edited the writing. All the authors read, critically reviewed and approved the final version.

FUNDING

This work was supported by the Government of the Cesar Department through the Administrative Department of Science, Technology and Innovation (Colciencias) (Grant No. 681, 2014).

CONFLICT OF INTEREST

The authors declare no conflicts of interest.

DATA AVAILABILITY STATEMENT

All relevant data are available from an online repository or repositories (https://data.mendeley.com/datasets/z9w7d7gw9n/1).

REFERENCES

Blatchley, E. R., Shen, C., Scheible, O. K., Robinson, J. P., Ragheb, K., Bergstrom, D. E. & Rokjer, D. 2008 Validation of large-scale, monochromatic UV disinfection systems for drinking water using dyed microspheres. *Water Research* **42** (3), 677–688. https://doi.org/10.1016/j.watres.2007.08.019.

Britt, A. B. 1996 DNA damage and repair in plants. *Annual Review of Plant Physiology and Plant Molecular Biology* **47** (1), 75–100. https://doi.org/10.1146/annurev.arplant.47.1.75.

Chatterley, C. & Linden, K. G. 2009 UV-LED irradiation technology for point-of-use water disinfection. *Proceedings of the Water Environment Federation* **2009** (1), 222–225. https://doi.org/10.2175/193864709793848176.

Chatterley, C. & Linden, K. 2010 Demonstration and evaluation of germicidal UV-LEDs for point-of-use water disinfection. *Journal of Water and Health* **8** (3), 479–486. https://doi.org/10.2166/wh.2010.124.

Chevremont, A. C., Farnet, A. M., Coulomb, B. & Boudenne, J. L. 2012 Effect of coupled UV-A and UV-C LEDs on both microbiological and chemical pollution of urban wastewaters. *Science of the Total Environment* **426**, 304–310. https://doi.org/10.1016/j.scitotenv.2012.03.043.

Dang, C., Xia, Y., Zheng, M., Liu, T., Liu, W., Chen, Q. & Ni, J. 2020 Metagenomic insights into the profile of antibiotic resistomes in a large drinking water reservoir. *Environment International* **136**, 105449. https://doi.org/10.1016/j.envint.2019.105449.

Essen, L. O. & Klar, T. 2006 Light-driven DNA repair by photolyases. **63**, 1266–1277. https://doi.org/10.1007/s00018-005-5447-y.

Foka, F. E. T., Yah, C. S. & Agbortabot Bissong, M. E. 2018 Physico-chemical properties and microbiological quality of borehole water in four crowded areas of Benin City, Nigeria, during rainfalls. *Shiraz E-Medical Journal* **19** (11), 1–8. https://doi.org/10.5812/semj.68911.

Giese, N. & Darby, J. 2000 Sensitivity of microorganisms to different wavelengths of UV light: implications on modeling of medium pressure UV systems. *Water Research* **34** (16), 4007–4013. https://doi.org/10.1016/S0043-1354(00)00172-X.

Guo, M., Huang, J., Hu, H. & Liu, W. 2011 Growth and repair potential of three species of bacteria in reclaimed wastewater after UV disinfection. *Biomedical and Environmental Sciences* **24** (4), 400–407. https://doi.org/10.3967/0895-3988.2011.04.011.

Hu, J. Y., Chu, X. N., Quek, P. H., Feng, Y. Y. & Tan, X. L. 2005 Repair and regrowth of *Escherichia coli* after low- and medium-pressure ultraviolet disinfection. *Water Science and Technology: Water Supply* **5** (5), 101–108. https://doi.org/10.2166/ws.2005.0044.

Li, G. Q., Wang, W. L., Huo, Z. Y., Lu, Y. & Hu, H. Y. 2017 Comparison of UV-LED and low pressure UV for water disinfection: photoreactivation and dark repair of *Escherichia coli*. *Water Research* **126**, 134–143. https://doi.org/10.1016/j.watres.2017.09.030.

Mossel, D. A. A., Corry, J. E. L., Struijk, C. B. & Baird, R. M. 1995 *Essentials of the Microbiology of Foods: A Textbook for Advanced Studies*. John Wiley and Sons, New York.

Nakahashi, M., Mawatari, K., Hirata, A., Maetani, M., Shimohata, T., Uebanso, T., Hamada, Y., Akutagawa, M., Kinouchi, Y. & Takahashi, A. 2014 Simultaneous irradiation with different wavelengths of ultraviolet light has synergistic bactericidal effect on *Vibrio parahaemolyticus*. *Photochemistry and Photobiology* **90** (6), 1397–1403. https://doi.org/10.1111/php.12309.

Nyangaresi, P. O., Qin, Y., Chen, G., Zhang, B., Lu, Y. & Shen, L. 2018 Effects of single and combined UV-LEDs on inactivation and subsequent reactivation of E. coli in water disinfection. *Water Research* **147**, 331–341. https://doi.org/10.1016/j.watres.2018.10.014.

Oguma, K., Kita, R., Sakai, H., Murakami, M. & Takizawa, S. 2013 Application of UV light emitting diodes to batch and flow-through water disinfection systems. *Desalination* **328**, 24–30. https://doi.org/10.1016/j.desal.2013.08.014.

Quek, P. H. & Hu, J. 2008 Influence of photoreactivating light intensity and incubation temperature on photoreactivation of *Escherichia coli* following LP and MP UV disinfection. *Journal of Applied Microbiology* **105** (1), 124–133. https://doi.org/10.1111/j.1365-2672.2008.03723.x.

Rastogi, R. P., Kumar, A., Tyagi, M. B. & Sinha, R. P. 2010 Molecular mechanisms of ultraviolet radiation-Induced DNA damage and repair. *Journal of Nucleic Acids* **2010**, 1–32. https://doi.org/10.4061/2010/592980.

Rattanakul, S. & Oguma, K. 2018 Inactivation kinetics and efficiencies of UV-LEDs against *Pseudomonas aeruginosa*, *Legionella pneumophila*, and surrogate microorganisms. *Water Research* **130**, 31–37. https://doi.org/10.1016/j.watres.2017.11.047.

Song, K., Taghipour, F. & Mohseni, M. 2018 Microorganisms inactivation by continuous and pulsed irradiation of ultraviolet light-emitting diodes (UV-LEDs). *Chemical Engineering Journal* **343**, 362–370. https://doi.org/10.1016/j.cej.2018.03.020.

Voigt, A. M., Ciorba, P., Döhla, M., Exner, M., Felder, C., Lenz-Plet, F., Sib, E., Skutlarek, D., Schmithausen, R. M. & Faerber, H. A. 2020 The investigation of antibiotic residues, antibiotic resistance genes and antibiotic-resistant organisms in a drinking water reservoir system in Germany. *International Journal of Hygiene and Environmental Health* **224**, 113449. https://doi.org/10.1016/j.ijheh.2020.113449.

Würtele, M. A., Kolbe, T., Lipsz, M., Külberg, A., Weyers, M., Kneissl, M. & Jekel, M. 2011 Application of GaN-based ultraviolet-C light emitting diodes – UV LEDs – for water disinfection. *Water Research* **45** (3), 1481–1489. https://doi.org/10.1016/j.watres.2010.11.015.

Xiao, Y., Chu, X. N., He, M., Liu, X. C. & Hu, J. Y. 2018 Impact of UVA pre-radiation on UVC disinfection performance: inactivation, repair and mechanism study. *Water Research* **141**, 279–288. https://doi.org/10.1016/j.watres.2018.05.021.

Zhang, L. W., Li, M. & Wu, Q. Y. 2007 Influence of ultraviolet-C on structure and function of *Synechococcus* sp. PCC 7942 photolyase. *Biochemistry* **72** (5), 540–544. https://doi.org/10.1134/S0006297907050100.

Zimmer, J. L. & Slawson, R. M. 2002 Potential repair of *Escherichia coli* DNA following exposure to UV radiation from both medium- and low-pressure UV sources used in drinking water treatment. *Applied and Environmental Microbiology* **68** (7), 3293–3299. https://doi.org/10.1128/AEM.68.7.3293-3299.2002.

First received 10 June 2021; accepted in revised form 30 September 2021. Available online 14 October 2021